TECHNICAL ARTICLE

Crystal structure of dutasteride (Avodart), $C_{27}H_{20}F_6N_2O_2$

James A. Kaduk,[1,a] Cyrus E. Crowder,[2] Kai Zhong,[2] Timothy G. Fawcett,[2] and Matthew R. Suchomel[3]
[1]*Illinois Institute of Technology, 3101 S. Dearborn Street, Chicago, Illinois 60616*
[2]*ICDD, 12 Campus Blvd., Newtown Square, Pennsylvania 19073-3273*
[3]*Advanced Photon Source, Argonne National Laboratory, 9700 S. Cass Avenue, Argonne, Illinois 60439*

(Received 9 March 2014; accepted 22 May 2014)

Commercial dutasteride crystallizes in the orthorhombic space group $P2_12_12_1$ (#19), with $a = 7.587\,44(3)$, $b = 9.960\,80(5)$, $c = 33.500\,42(12)$ Å, $V = 2531.862(17)$ Å^3, and $Z = 4$. The structure was solved and refined using synchrotron powder diffraction data, Rietveld, and density functional techniques. The most prominent feature of the structure is a zigzag chain of strong N–H···O = C hydrogen bonds along the *a*-axis. The powder pattern has been submitted to ICDD for inclusion in future releases of the Powder Diffraction File™. © *2014 International Centre for Diffraction Data.*
[doi:10.1017/S088571561400061X]

Key words: dutasteride, powder diffraction, Rietveld, density functional

I. INTRODUCTION

Dutasteride (Avodart), an oral pharmaceutical approved by the US Food and Drug Administration (USFDA) for the treatment of moderate to severe benign prostatic hyperplasia (BPH) in men, is a potent, selective, and irreversible inhibitor of type 1 and type 2 5α-reductase (5AR) (Andriole *et al.*, 2004). 5AR is the enzyme which catalyzes the formation of androgen dihydrotestosterone (DHT) from its precursor testosterone intracellularly (Clark *et al.*, 2004), and therefore is critical for the growth of the prostate gland. Dutasteride has the systematic name (5α,17β)-*N*-{2,5-bis(trifluoromethyl) phenyl}-3-oxo-4-azaandrost-1-ene-17-carboxamide. A two-dimensional (2D) structural diagram is shown in Figure 1.

The presence of high-quality reference powder patterns in the Powder Diffraction File (PDF) (ICDD, 2013) is important for phase identification, particularly by pharmaceutical, forensic, and law enforcement scientists. The crystal structures of a significant fraction of the largest dollar volume pharmaceuticals have not been published, and thus calculated powder patterns are not present in the PDF-4 Organics database. Sometimes experimental patterns are reported, but they are generally of low quality. Accordingly, a collaboration among the ICDD, IIT, Poly Crystallography Inc., and Argonne National Laboratory has been established to measure high-quality synchrotron powder patterns of commercial pharmaceutical ingredients, to include these reference patterns in the PDF, and determine the crystal structures of these Active Pharmaceutical Ingredients (APIs).

Even when the crystal structure of an API is reported, the single-crystal structure was often determined at low temperature. Most powder measurements are performed at ambient conditions. Thermal expansion (often anisotropic) means that the peak positions calculated from a low-temperature single-crystal structure often differ from those measured at ambient conditions. These peak shifts can result in failure of default search/match algorithms to identify a phase, even when it is present in the sample. High-quality reference patterns measured at ambient conditions are thus critical for easy identification of APIs using standard powder diffraction practices.

II. EXPERIMENTAL

The dutasteride 99% was a commercial material, purchased from AK Scientific (Lot #LC24263), and was used as-received. The white powder was packed into a 1.5 mm diameter Kapton capillary, and rotated during the experiment at ~50 cycles s^{-1}. The powder pattern was measured at beam line 11-BM (Lee *et al.*, 2008; Wang *et al.*, 2008) of the Advanced Photon Source at the Argonne National Laboratory using a wavelength of 0.413 891 Å at 296 K from 0.5° to 50° 2θ with a step size of 0.001° and a counting time of 0.1 s step^{-1}. The pattern was indexed using FOX (Favre-Nicolin and Černý, 2002) and N-TREOR (Altomare *et al.*, 2000) in EXPO2013 (Altomare *et al.*, 2009, 2013). The systematic absences determined the space group to be $P2_12_12_1$ (#19) (a common space group for

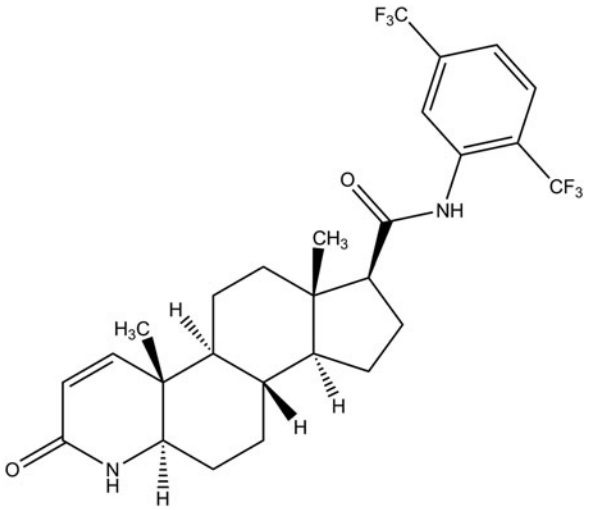

Figure 1. Molecular structure of dutasteride.

[a]Author to whom correspondence should be addressed. Electronic mail: kaduk@polycrystallography.com

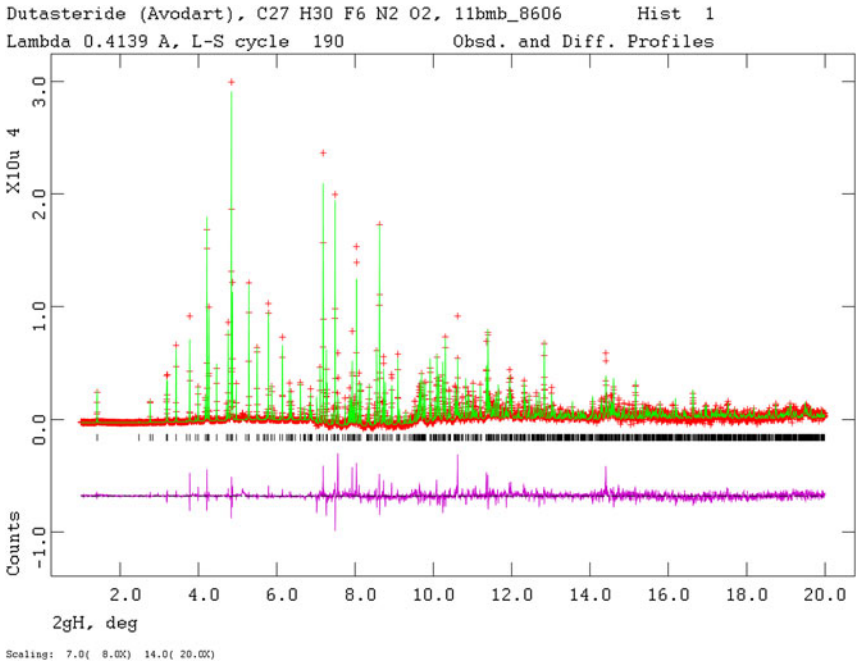

Figure 2. (Color online) Observed, calculated, and difference patterns of dutasteride. The red crosses represent the observed data points, the green solid line the calculated pattern, and the magenta line the difference (observed–calculated) pattern. The vertical scale is multiplied by a factor of 8 above 7° 2θ and by a factor of 20 above 14°.

TABLE I. Rietveld refined structure of dutasteride. Space group $P2_12_12_1$ (#19), with $a = 7.587\ 44(3)$, $b = 9.960\ 80(5)$, $c = 33.500\ 42(12)$ Å, $V = 2531.862(17)$ Å^3, and $Z = 4$.

Name	X	Y	Z	U_{iso}*100
C1	0.8883(9)	0.6482(8)	0.517 21(39)	3.70(10)
N2	0.7255(9)	0.6014(8)	0.519 15(28)	3.70(10)
C3	0.6929(9)	0.4623(8)	0.528 10(23)	3.70(10)
C4	0.8098(10)	0.4188(7)	0.563 42(23)	3.70(10)
C5	0.9972(11)	0.4468(10)	0.550 48(32)	3.70(10)
C6	1.0305(9)	0.5551(10)	0.528 67(35)	3.70(10)
O7	0.9219(8)	0.7704(8)	0.506 68(26)	3.70(10)
C8	0.4984(13)	0.4416(10)	0.536 16(30)	3.70(10)
C9	0.4714(12)	0.2883(11)	0.541 89(31)	3.70(10)
C10	0.5826(10)	0.2353(8)	0.578 00(26)	3.70(10)
C11	0.7762(10)	0.2661(7)	0.570 53(26)	3.70(10)
C12	0.7743(12)	0.4890(12)	0.603 13(27)	3.47(33)
C13	0.5588(10)	0.0812(9)	0.581 86(26)	3.70(10)
C14	0.6639(9)	0.0234(8)	0.616 30 (25)	3.70(10)
C15	0.8604(11)	0.0455(9)	0.606 94(32)	3.70(10)
C16	0.8969(11)	0.1973(9)	0.600 96(32)	3.70(10)
C17	0.6126(14)	0.0819(12)	0.656 53(30)	3.47(33)
C18	0.3668(11)	0.0319(11)	0.590 93 (33)	3.70(10)
C19	0.4027(12)	−0.1143(10)	0.605 48(34)	3.70(10)
C20	0.5998(10)	−0.1229(8)	0.614 78(25)	3.70(10)
C21	0.6501(10)	−0.2050(10)	0.650 49(29)	6.60(27)
O22	0.8026(10)	−0.2076(9)	0.662 53(25)	6.60(27)
N23	0.5279(12)	−0.2998(10)	0.661 51(29)	6.60(27)
C24	0.5488(9)	−0.4036(6)	0.690 86(20)	4.78(23)
C25	0.4212(7)	−0.5033(7)	0.694 37(21)	4.78(23)
C26	0.4438(9)	−0.6071(6)	0.721 73(22)	4.78(23)
C27	0.5939(10)	−0.6111(7)	0.745 58(19)	4.78(23)
C28	0.7215(7)	−0.5114(8)	0.742 07 (18)	4.78(23)
C29	0.6989(7)	−0.4076(7)	0.714 71 (20)	4.78(23)
H30	0.3558(11)	−0.6759(7)	0.724 15(32)	6.21(30)
H31	0.6095(14)	−0.6827(9)	0.764 44(27)	6.21(30)
H32	0.7869(9)	−0.3388(9)	0.712 29(30)	6.21(30)
C33	0.2510(12)	−0.4972(10)	0.668 12(31)	13.56(17)
F34	0.1784(11)	−0.3875(9)	0.673 22(28)	13.56(17)
F35	0.1434(11)	−0.5911(10)	0.677 10(25)	13.56(17)
F36	0.2903(9)	−0.5126(10)	0.631 89(25)	13.56(17)

Continued

TABLE I. Continued

Name	X	Y	Z	U_{iso}*100
C37	0.8765(11)	−0.5190(10)	0.769 83 (27)	13.56(17)
F38	0.920 442	−0.400 170	0.783 232	13.56(17)
F39	0.849 823	−0.588 305	0.800 705	13.56(17)
F40	1.014 583	−0.555 718	0.755 177	13.56(17)
H41	0.621 970	0.659 250	0.510 680	4.82(13)
H42	0.736 550	0.402 490	0.505 340	4.82(13)
H43	1.109 560	0.396 960	0.566 510	4.82(13)
H44	1.166 290	0.597 010	0.525 240	4.82(13)
H45	0.786 090	0.599 840	0.600 260	4.52(43)
H46	0.872 000	0.466 380	0.628 370	4.52(43)
H47	0.644 370	0.470 440	0.617 070	4.52(43)
H48	0.426 050	0.471 100	0.511 450	4.82(13)
H49	0.449 860	0.490 430	0.563 380	4.82(13)
H50	0.504 790	0.230 540	0.515 650	4.82(13)
H51	0.331 990	0.262 850	0.549 170	4.82(13)
H52	0.538 390	0.275 530	0.605 140	4.82(13)
H53	0.822 260	0.214 070	0.542 980	4.82(13)
H54	0.620 570	0.030 490	0.554 880	4.82(13)
H55	0.904 150	−0.011 900	0.583 400	4.82(13)
H56	0.942 130	0.006 020	0.634 980	4.82(13)
H57	0.881 270	0.247 030	0.632 710	4.82(13)
H58	1.038 360	0.207 950	0.596 740	4.72(13)
H59	0.629 110	0.182 380	0.660 640	4.52(43)
H60	0.680 750	0.026 830	0.682 380	4.52(43)
H61	0.466 420	0.056 760	0.663 750	4.52(43)
H62	0.305 990	0.014 090	0.557 310	4.82(13)
H63	0.295 630	0.076 960	0.606 340	4.82(13)
H64	0.376 400	−0.202 660	0.580 200	4.82(13)
H65	0.318 320	−0.143 090	0.628 070	4.82(13)
H66	0.677 290	−0.176 500	0.589 000	4.82(13)
H67	0.4182 20	−0.308 100	0.648 380	8.58(36)

chiral organic compounds), which was confirmed by successful solution and refinement of the structure. A dutasteride molecule was built and its conformation optimized using Spartan '10 (Wavefunction, 2011). The hydrogen atoms were removed, and it was saved as a mol2 file and converted into a MOPAC

https://doi.org/10.1017/S088571561400061X Published online by Cambridge University Press

TABLE II. Density functional optimized structure of dutasteride. Space group $P2_12_12_1$ (#19), with a=7.587 435, b = 9.960 79, c = 33.500 43 Å, V = 2531.862 Å^3, and Z = 4.

Name	X	Y	Z	U_{iso}
C1	0.889 15	0.653 11	0.518 35	0.037 00
N2	0.724 57	0.604 01	0.522 28	0.037 00
C3	0.694 44	0.462 46	0.531 31	0.037 00
C4	0.813 32	0.415 39	0.566 28	0.037 00
C5	0.999 99	0.453 91	0.554 29	0.037 00
C6	1.033 56	0.563 79	0.532 23	0.037 00
O7	0.917 37	0.768 24	0.504 91	0.037 00
C8	0.498 83	0.434 58	0.537 49	0.037 00
C9	0.471 33	0.283 87	0.543 33	0.037 00
C10	0.584 38	0.227 88	0.577 47	0.037 00
C11	0.783 64	0.260 74	0.571 48	0.037 00
C12	0.775 53	0.492 12	0.605 41	0.034 70
C13	0.562 25	0.075 98	0.581 81	0.037 00
C14	0.665 75	0.016 86	0.617 53	0.037 00
C15	0.862 79	0.043 67	0.610 16	0.037 00
C16	0.898 74	0.195 04	0.604 18	0.037 00
C17	0.606 69	0.074 45	0.658 21	0.034 70
C18	0.375 92	0.017 10	0.585 81	0.037 00
C19	0.406 50	−0.126 39	0.602 68	0.037 00
C20	0.605 65	−0.132 55	0.614 36	0.037 00
C21	0.659 69	−0.218 49	0.649 85	0.066 00
O22	0.807 43	−0.211 13	0.664 32	0.066 00
N23	0.532 99	−0.308 30	0.663 75	0.066 00
C24	0.555 60	−0.410 46	0.692 03	0.047 80
C25	0.426 99	−0.512 79	0.696 42	0.047 80
C26	0.449 13	−0.614 57	0.724 65	0.047 80
C27	0.597 28	−0.617 61	0.749 04	0.047 80
C28	0.722 68	−0.516 17	0.745 07	0.047 80
C29	0.704 56	−0.414 11	0.716 99	0.047 80
H30	0.348 28	−0.690 61	0.728 01	0.062 10
H31	0.614 63	−0.696 09	0.771 01	0.062 10
H32	0.803 98	−0.337 46	0.713 41	0.062 10
C33	0.262 19	−0.513 12	0.671 48	0.135 60
F34	0.155 62	−0.405 82	0.679 65	0.135 60
F35	0.164 09	−0.625 17	0.676 08	0.135 60
F36	0.298 42	−0.503 87	0.631 21	0.135 60
C37	0.882 97	−0.517 28	0.771 68	0.135 60
F38	0.947 31	−0.391 73	0.778 51	0.135 60
F39	0.846 41	−0.572 14	0.807 99	0.135 60
F40	1.018 16	−0.589 94	0.755 77	0.135 60
H41	0.621 97	0.659 25	0.510 68	0.048 20
H42	0.736 55	0.402 49	0.505 34	0.048 20
H43	1.109 56	0.396 96	0.566 51	0.048 20
H44	1.166 29	0.597 01	0.525 24	0.048 20
H45	0.786 09	0.599 84	0.600 26	0.045 20
H46	0.872 00	0.466 38	0.628 37	0.045 20
H47	0.644 37	0.470 44	0.617 07	0.045 20
H48	0.426 05	0.471 10	0.514 55	0.048 20
H49	0.449 86	0.490 43	0.563 38	0.048 20
H50	0.504 79	0.230 54	0.515 65	0.048 20
H51	0.331 99	0.262 85	0.549 17	0.048 20
H52	0.538 39	0.275 53	0.605 14	0.048 20
H53	0.822 26	0.214 07	0.542 98	0.048 20
H54	0.620 57	0.030 49	0.554 88	0.048 20
H55	0.904 15	−0.011 90	0.583 40	0.048 20
H56	0.942 13	0.006 02	0.634 98	0.048 20
H57	0.881 27	0.247 03	0.632 71	0.048 20
H58	1.038 36	0.207 95	0.596 74	0.047 20
H59	0.629 11	0.182 38	0.660 64	0.045 20
H60	0.680 75	0.026 83	0.682 38	0.045 20
H61	0.466 42	0.056 76	0.663 75	0.045 20
H62	0.305 99	0.014 09	0.557 31	0.048 20
H63	0.295 63	0.076 96	0.606 34	0.048 20
H64	0.376 40	−0.202 66	0.580 20	0.048 20
H65	0.318 32	−0.143 09	0.628 07	0.048 20
H66	0.677 29	−0.176 50	0.589 00	0.048 20
H67	0.418 22	−0.308 10	0.648 38	0.085 80

file using OpenBabel (O'Boyle *et al.*, 2011). The structure was solved with EXPO2013 (Altomare *et al.*, 2009, 2013) using simulated annealing.

The Rietveld refinement was carried out using GSAS (Larson and Von Dreele, 2004). Only the 1°–20° portion of the pattern was included in the refinement. The C_6H_3 phenyl group was refined as a rigid body, and all non-H bond distances and angles were subjected to restraints, based on a Mercury/Mogul Geometry Check (Bruno *et al.*, 2004; Sykes *et al.*, 2011) of the molecule. The Mogul average and standard deviation for each quantity were used as the restraint parameters. The restraints contributed 1.68% to the final χ^2. Isotropic displacement coefficients were refined, and grouped by chemical similarity. The U_{iso} of each hydrogen atom was constrained to be 1.3× that of the heavy atom to which it is attached. The peak profiles were described using profile function #4, which includes the Stephens (1999) anisotropic strain broadening model. The background was modeled using a three-term shifted Chebyshev polynomial and a four-term diffuse scattering function to describe the scattering from the Kapton capillary and any amorphous content of the sample. The final refinement of 104 variables using 19 087 observations yielded the residuals $wRp = 0.1207$, $Rp = 0.0971$, and $\chi^2 = 3.603$. The largest peak (0.44 Å from F34) and hole (0.72 Å from F38) in the difference Fourier map were 0.61 and −0.45 eÅ^{-3}, respectively. The Rietveld plot is included as in Figure 2. The largest errors are in the positions and shapes of low-angle peaks, and probably indicate non-uniformity in the crystallites. A trace of an unidentified impurity phase was present.

A density functional geometry optimization (fixed experimental unit cell) was carried out using CRYSTAL09 (Dovesi *et al.*, 2005). The basis sets for the H, C, N, and O atoms were those of Gatti *et al.* (1994), and the basis set for F was that of Nada *et al.* (1993). The calculation used eight k-points and the B3LYP functional.

III. RESULTS AND DISCUSSION

The refined atom coordinates of dutasteride are reported in Table I, and the coordinates from the density functional theory (DFT) optimization in Table II. The root-

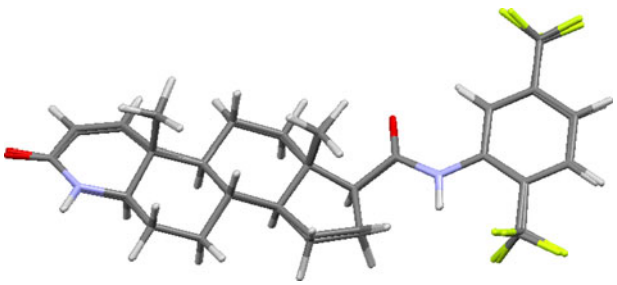

Figure 3. (Color online) Comparison of the Rietveld-refined and DFT-optimized structures of dutasteride. The RMS difference between the non-hydrogen atom positions is 0.14 Å.

https://doi.org/10.1017/S088571561400061X Published online by Cambridge University Press

mean-square (RMS) deviation of the non-hydrogen atoms is 0.14 Å, and the maximum deviation is 0.33 Å, in the CF_3 groups (Figure 3). The relatively large displacement coefficient of the CF_3 groups suggests that some disorder might be present, but sorting it out is beyond the scope of a powder experiment. The discussion of the geometry uses the DFT-optimized structure. The asymmetric unit (with atom numbering) is illustrated in Figure 4, and the crystal structure is presented in Figure 5.

Almost all bond distances, angles, and torsion angles fall within the normal ranges indicated by a Mercury Geometry Check. Only the bonds C1–C6 at 1.486 Å [average = 1.430 (22), *Z*-score = 2.57] and C21–N23 at 1.393 Å [average = 1.350(19), *Z*-score = 2.28], the angles C8–C3–C4 = 114.1 [average = 112.9(6), *Z*-score = 2.00] C19–C20–C21 = 118.6 [average = 114.1(19), *Z*-score = 2.42] C27–C28–C29 = 121.8 [average = 117.6(19), *Z*-score = 2.16], and the torsion angles O22–C21–C20–C19 and C19–C20–C21–N23 fall slightly outside the normal ranges. There are no voids in the crystal structure.

The most prominent feature of the crystal structure is the N2–H41···O7 hydrogen bonds (Table III). They form a zigzag chain parallel to the *a*-axis (Figure 6). The graph set is *C*1,1 (4). This is a chain of four atoms containing one donor and one acceptor (Etter, 1990; Bernstein *et al.*, 1995; Shields, *et al.*, 2000). The Mulliken overlap population indicates that these hydrogen bonds are reasonably strong. The average N···O for such hydrogen bonds in the CSD is 2.89(16) Å and the average N–H···O angle is 155(25)°; so these hydrogen bonds are shorter and more linear than the average. The Mulliken overlap populations suggest that there are weak intramolecular C–H···O and C–H···F interactions. Perhaps surprisingly, the amide N23–H67 does not participate in hydrogen bonds; the shortest potential (intramolecular) N23···F contacts are 2.855 and 3.071 Å, to F36 and F34, respectively, but these seem not to represent the real hydrogen bonds. Other than the hydrogen bonds, the crystal structure is dominated by van der Waals contacts.

The Bravais–Friedel–Donnay–Harker (Bravais, 1866; Friedel, 1907; Donnay and Harker, 1937) morphology

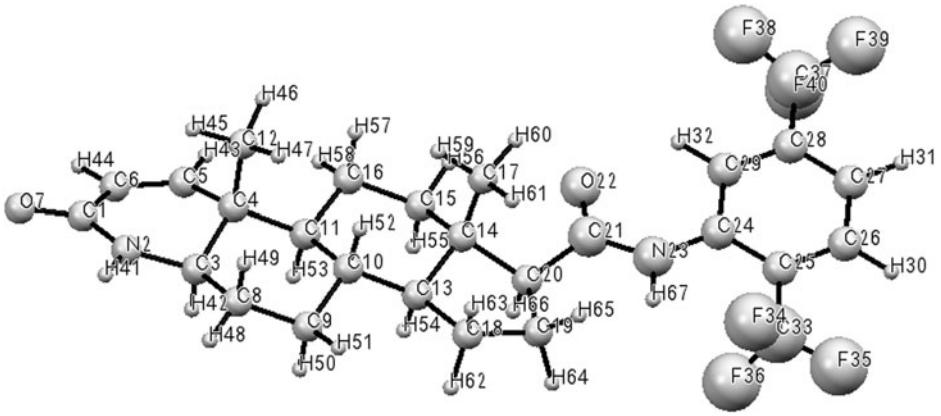

Figure 4. The asymmetric unit of dutasteride, with the atom numbering.

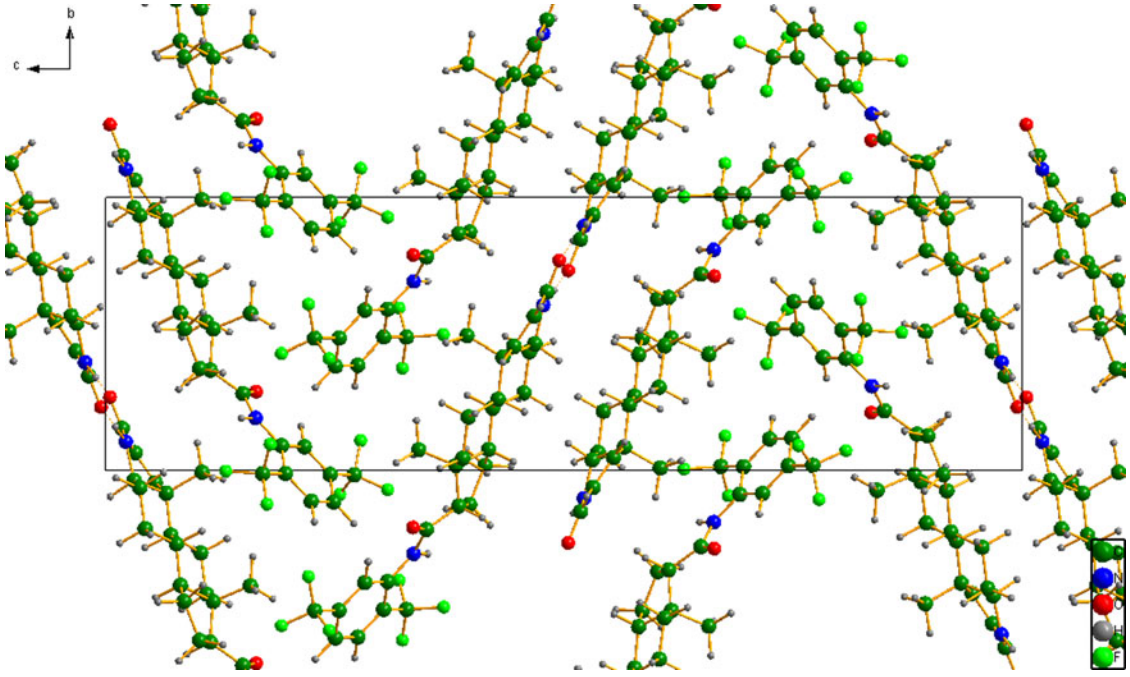

Figure 5. (Color online) Crystal structure of dutasteride. The view is down the *a*-axis.

https://doi.org/10.1017/S088571561400061X Published online by Cambridge University Press

TABLE III. Hydrogen bonds in dutasteride.

D–H···A	D–H (Å)	H···A (Å)	D···A (Å)	D–H···A (°)	Overlap (*e*)
N2–H41···O7	1.030	1.790	2.807	169.0	0.074
C29–H32···O22	1.080	2.071	2.795	121.8	0.023
C26–H30···F35	1.083	2.325	2.709	98.7	0.005
C37–H31···F39	1.082	2.480	2.771	93.8	0.005

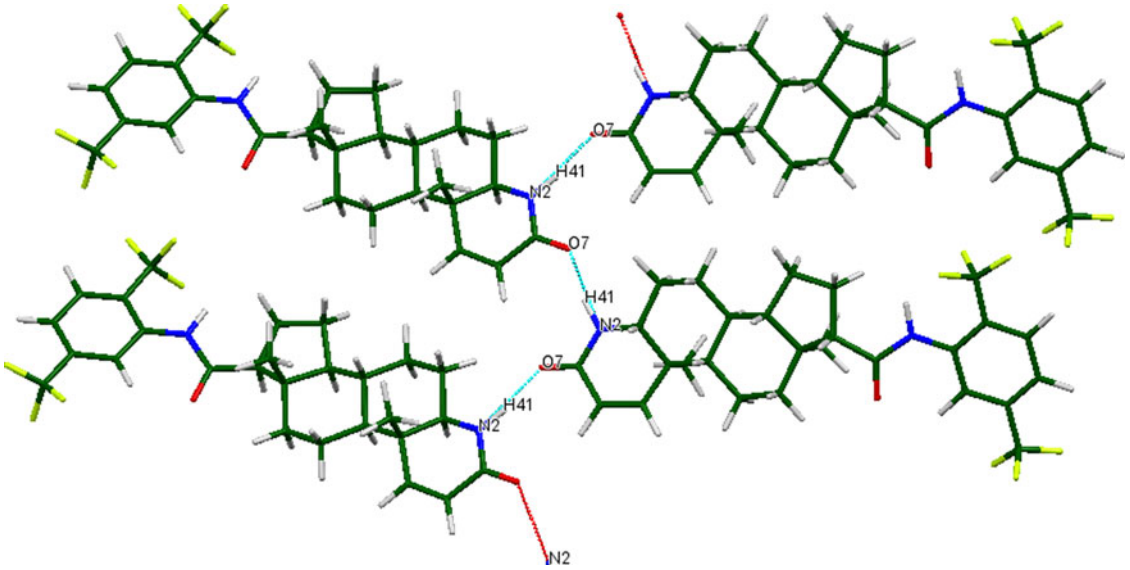

Figure 6. (Color online) The N2–H41···O7 hydrogen bond pattern.

suggests that we might expect platy morphology for dutasteride, with {001} as the principal faces. The texture index, modeled using second-order spherical harmonics, was 1.033.

The powder pattern of dutasteride has been submitted to ICDD for inclusion in future releases of the Powder Diffraction File.

ACKNOWLEDGEMENTS

Use of the Advanced Photon Source at the Argonne National Laboratory was supported by the US Department of Energy, Office of Science, Office of Basic Energy Sciences, under Contract No. DE-AC02-06CH11357. This work was partially supported by the International Centre for Diffraction Data. We thank Lynn Ribaud for his assistance in data collection, and Silvina Pagola for her participation in the early stages of this project.

Supplementary Materials and Methods

The supplementary material refered to in this paper can befound online at journals.cambridge.org/pdj.

Altomare, A., Giacovazzo, C., Guagliardi, A., Moliterni, A. G., Rizzi, R., and Werner, P. E. (**2000**). "New techniques for indexing: N-TREOR in EXPO," J. Appl. Crystallogr. **33**(4), 1180–1186.

Altomare, A., Camalli, M., Cuocci, C., Giacovazzo, C., Moliterni, A., and Rizzi, R. (**2009**). "EXPO2009: structure solution by powder data in direct and reciprocal space," J. Appl. Crystallogr. **42**(6), 1197–1202.

Altomare, A., Cuocci, C., Giacovazzo, C., Moliterni, A., Rizzi, R., Corriero, N., and Falcicchio, A. (**2013**). "EXPO2013: a kit of tools for phasing crystal structures from powder data," J. Appl. Crystallogr. **46**(4), 1231–1235.

Andriole, G., Bruchovsky, N., Chung, L. W., Matsumoto, A. M., Rittmaster, R., Roehrborn, C., Russell, D., and Tindall, D. (**2004**). "Dihydrotestosterone and the prostate: the scientific rationale for 5α-reductase inhibitors in the treatment of benign prostate hyperplasia," J. Urol. **172**, 1399–1403.

Bernstein, J., Davis, R. E., Shimoni, L., and Chang, N. L. (**1995**). "Patterns in hydrogen bonding: functionality and graph set analysis in crystals," Angew. Chem. Int. Ed. Engl. **34**(15), 1555–1573.

Bravais, A. (**1866**). *Etudes Cristallographiques* (Gathier Villars, Paris).

Bruno, I. J., Cole, J. C., Kessler, M., Luo, J., Motherwell, W. D. S., Purkis, L. H., Smith, B. R., Taylor, R., Cooper, R. I., Harris, S. E., and Orpen, A. G. (**2004**). "Retrieval of crystallographically-derived molecular geometry information," J. Chem. Inf. Sci. **44**, 2133–2144.

Clark, R. V., Hermann, D. J., Cunningham, G. R., Wilson, T. H., Morrill, B. B., and Hobbs, S. (**2004**). "Marked suppression of dihydrotestosterone in men with benign prostatic hyperplasia by dutasteride, a dual 5alpha-reductase inhibitor," J. Clin. Endocrinol. Metab. **89**, 2179–2184.

Donnay, J. D. H. and Harker, D. (**1937**). "A new law of crystal morphology extending the law of Bravais," Amer. Mineral. **22**, 446–467.

Dovesi, R., Orlando, R., Civalleri, B., Roetti, C., Saunders, V. R., and Zicovich-Wilson, C. M. (**2005**). "CRYSTAL: a computational tool for the *ab initio* study of the electronic properties of crystals," Zeit. Krist. **220**, 571–573.

Etter, M. C. (**1990**). "Encoding and decoding hydrogen-bond patterns of organic compounds," Acc. Chem. Res. **23**(4), 120–126.

Favre-Nicolin, V. and Černý, R. (**2002**). "FOX, Free objects for crystallography: a modular approach to *ab initio* structure determination from powder diffraction," J. Appl. Crystallogr. **35**, 734–743.

Friedel, G. (**1907**). "Etudes sur la loi de Bravais," Bull. Soc. Fr. Mineral. **30**, 326–455.

Gatti, C., Saunders, V. R., and Roetti, C. (**1994**). "Crystal-field effects on the topological properties of the electron-density in molecular crystals – the case of urea," J. Chem. Phys. **101**, 10686–10696.

ICDD (**2013**). PDF-4+ 2013 (Database), *International Centre for Diffraction Data*, edited by Dr. Soorya Kabekkodu (Newtown Square, PA, USA).

Larson, A. C. and Von Dreele, R. B. (**2004**). "General structure analysis system (GSAS)", Los Alamos National Laboratory Report LAUR 86–784.

Lee, P. L., Shu, D., Ramanathan, M., Preissner, C., Wang, J., Beno, M. A., Von Dreele, R. B., Ribaud, L., Kurtz, C., Antao, S. M., Jiao, X., and Toby, B. H. (**2008**). "A twelve-analyzer detector system for high-resolution powder diffraction," J. Synchrotron. Rad. **15**(5), 427–432.

Nada, R., Catlow, C. R. A., Pisani, C., and Orlando, R. (**1993**). "*Ab initio* Hartree–Fock perturbed-cluster study of neutral defects in LiF," Model. Simul. Mater. Sci. Eng. **1**, 165–187.

O'Boyle, N. M., Banck, M., James, C. A., Morley, C., Vandermeersch, T., and Hutchison, G. R. (**2011**). "OpenBabel: an open chemical toolbox," J. Chem. Inf. **3**, 1–14; doi: 10.1186/1758-2946-3-33.

Shields, G. P., Raithby, P. R., Allen, F. H., and Motherwell, W. S. (**2000**). "The assignment and validation of metal oxidation states in the Cambridge Structural Database," Acta Crystallogr. B: Struct. Sci., **56** (3), 455–465.

Stephens, P. W. (**1999**). "Phenomenological model of anisotropic peak broadening in powder diffraction," J. Appl. Crystallogr. **32**, 281–289.

Sykes, R. A., McCabe, P., Allen, F. H., Battle, G. M., Bruno, I. J., and Wood, P. A. (**2011**). "New software for statistical analysis of Cambridge Structural Database data," J. Appl. Crystallogr. **44**, 882–886.

Wang, J., Toby, B. H., Lee, P. L., Ribaud, L., Antao, S. M., Kurtz, C., Ramanathan, M., Von Dreele, R. B., and Beno, M. A. (**2008**). "A dedicated powder diffraction beamline at the Advanced Photon Source: commissioning and early operational results," Rev. Sci. Instrum. **79**, 085105.

Wavefunction, Inc. (**2011**). Spartan 10 Version 1.1.0, Wavefunction Inc., 18401 Von Karman Ave., Suite 370, Irvine CA 92612.

https://doi.org/10.1017/S088571561400061X Published online by Cambridge University Press